Electronic Supplementary Material (ESI) for RSC Advances.

SUPPORTING INFORMATION

Effects of the halogenido ligands to Kumada-coupling catalytic activity of $[Ni\{^tBuN(PPh_2)_2\text{-}\kappa^2P\}X_2]$, X = Cl, Br, I, complexes

Polydoros-Chrysovalantis Ioannou,[a] Radek Coufal,[b,c] Kalliopi Kakridi,[a] Catherine P. Raptopoulou,[d] Olga Trhlíková,[e] Vassilis Psycharis,*[d] Jiří Zedník,*[c] Panayotis Kyritsis,*[a] Jiří Vohlídal[c]

[a] Inorganic Chemistry Laboratory, Department of Chemistry, National and Kapodistrian University of Athens, Panepistimiopolis, Zografou, 15771 Athens, Greece

[b] Technical University of Liberec, Faculty of Health Studies, Department of Science and Research, Studentska 1402/2, CZ-461 17, Liberec 1, Czech Republic, radek.coufal@tul.cz

[c] Charles University, Faculty of Science, Department of Physical and Macromolecular Chemistry, Albertov 2030, CZ-128 43, Prague 2, Czech Republic

[d] Institute of Nanoscience and Nanotechnolgy, N.C.S.R. "Demokritos", Aghia Paraskevi 15310, Attiki, Greece

[e] Institute of Macromolecular Chemistry, v.v.i., Academy of Sciences of the Czech Republic, Heyrovský Sq. 2, 16206 Prague 6, Czech Republic

IR spectra

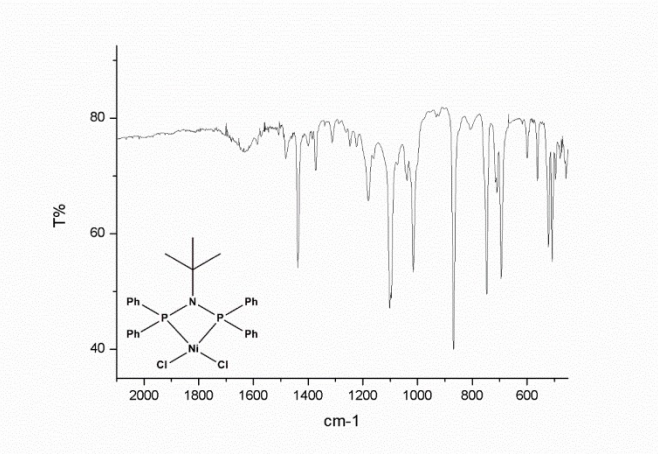

Figure S1. FT-IR spectrum of **[Ni(P,P)Cl$_2$]**. Selected bands (KBr, cm^{-1}): 1437 ν(P-Ph), 1180, 1101, 1015, 868 ν(P-N-P), 746, 694.

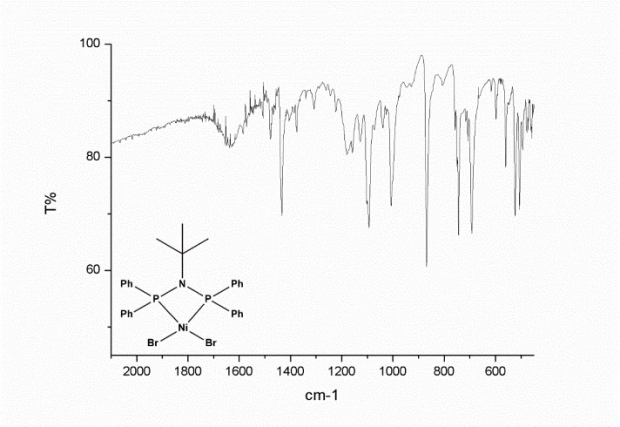

Figure S2. FT-IR spectrum of **[Ni(P,P)Br$_2$]**. Selected bands (KBr, cm^{-1}): 1477, 1433 ν(P-Ph), 1173, 1093, 1007, 868 ν(P-N-P), 744, 692.

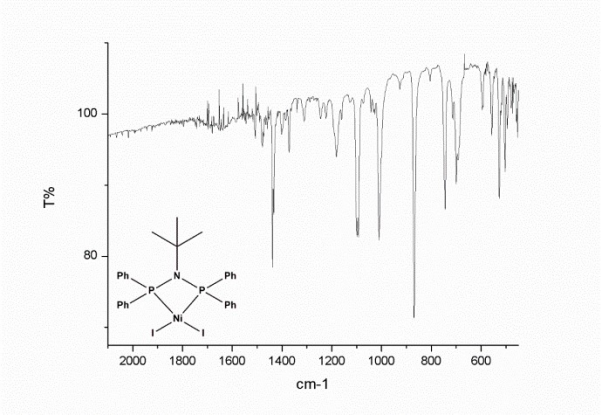

Figure S3. FT-IR spectrum of **[Ni(P,P)I$_2$]**. Selected bands (KBr, cm^{-1}): 1481, 1437 ν(P-Ph), 1370, 1180, 1098, 1009, 868 ν(P-N-P), 744, 700.

^{1}H and ^{13}C NMR spectra

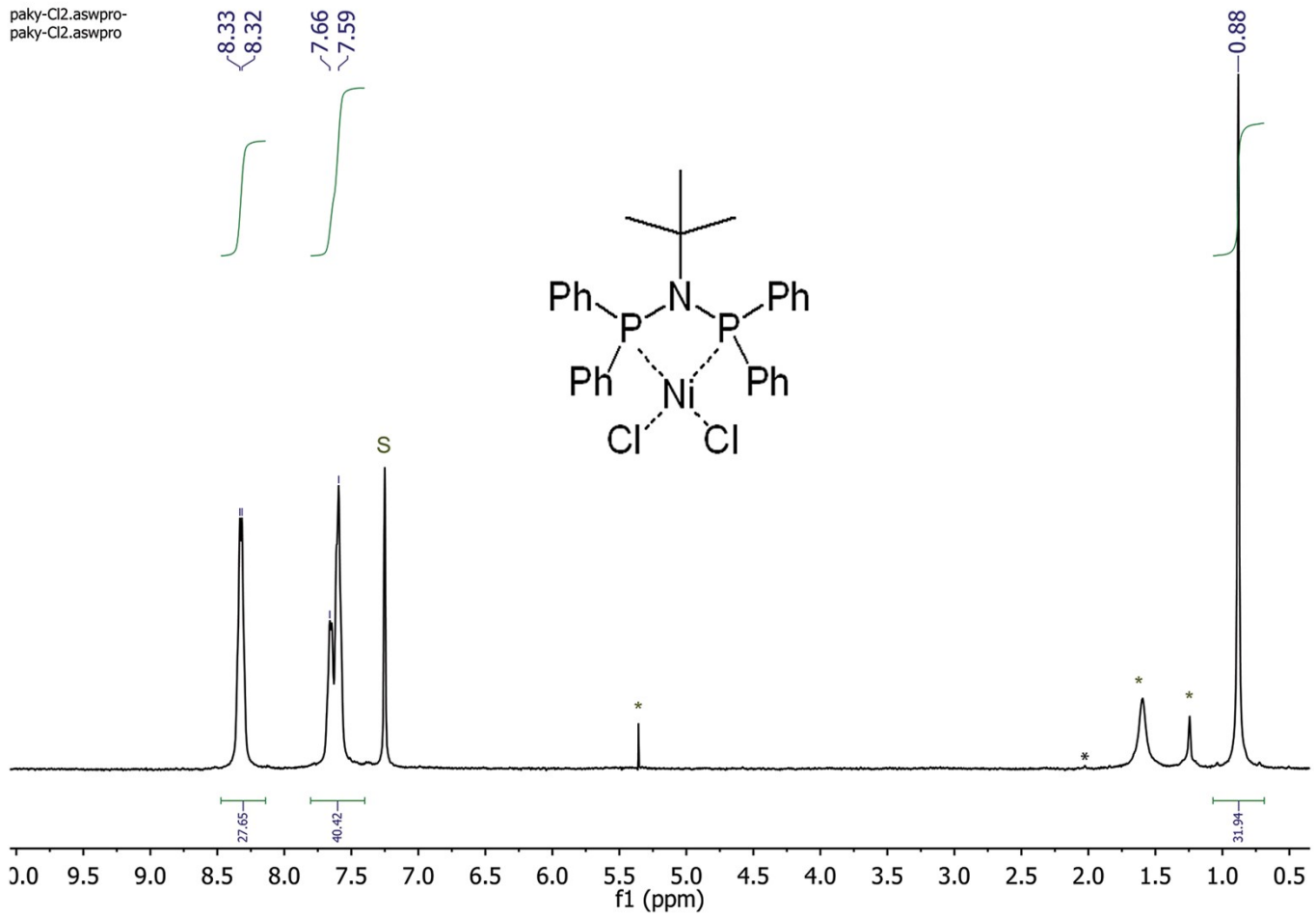

Figure S4. ^{1}H NMR (400 MHz, $CDCl_3$) spectrum of **[Ni(P,P)Cl$_2$]**. S – 7.25 ppm CH_3Cl (solvent signal), 5.27 ppm trace of dichloromethane, 2.10 ppm trace of acetone, 1.50 ppm trace of moisture, 1.25 ppm trace of hexane, all impurities are marked by an asterisk.

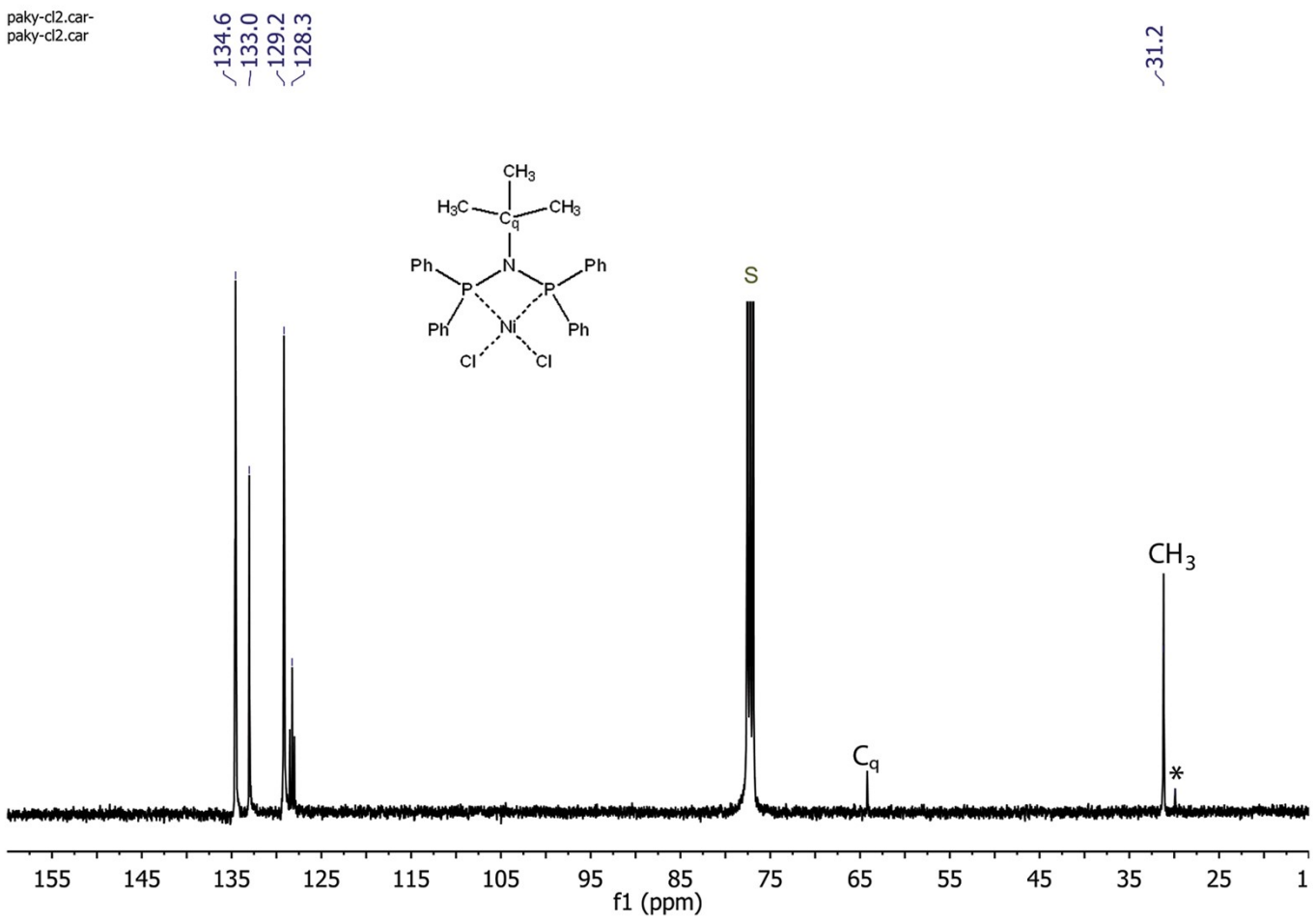

Figure S5. ^{13}C NMR (101 MHz, $CDCl_3$) spectrum of **[Ni(P,P)Cl$_2$],** S – solvent peak, residual trace of acetone is marked by an asterisk.

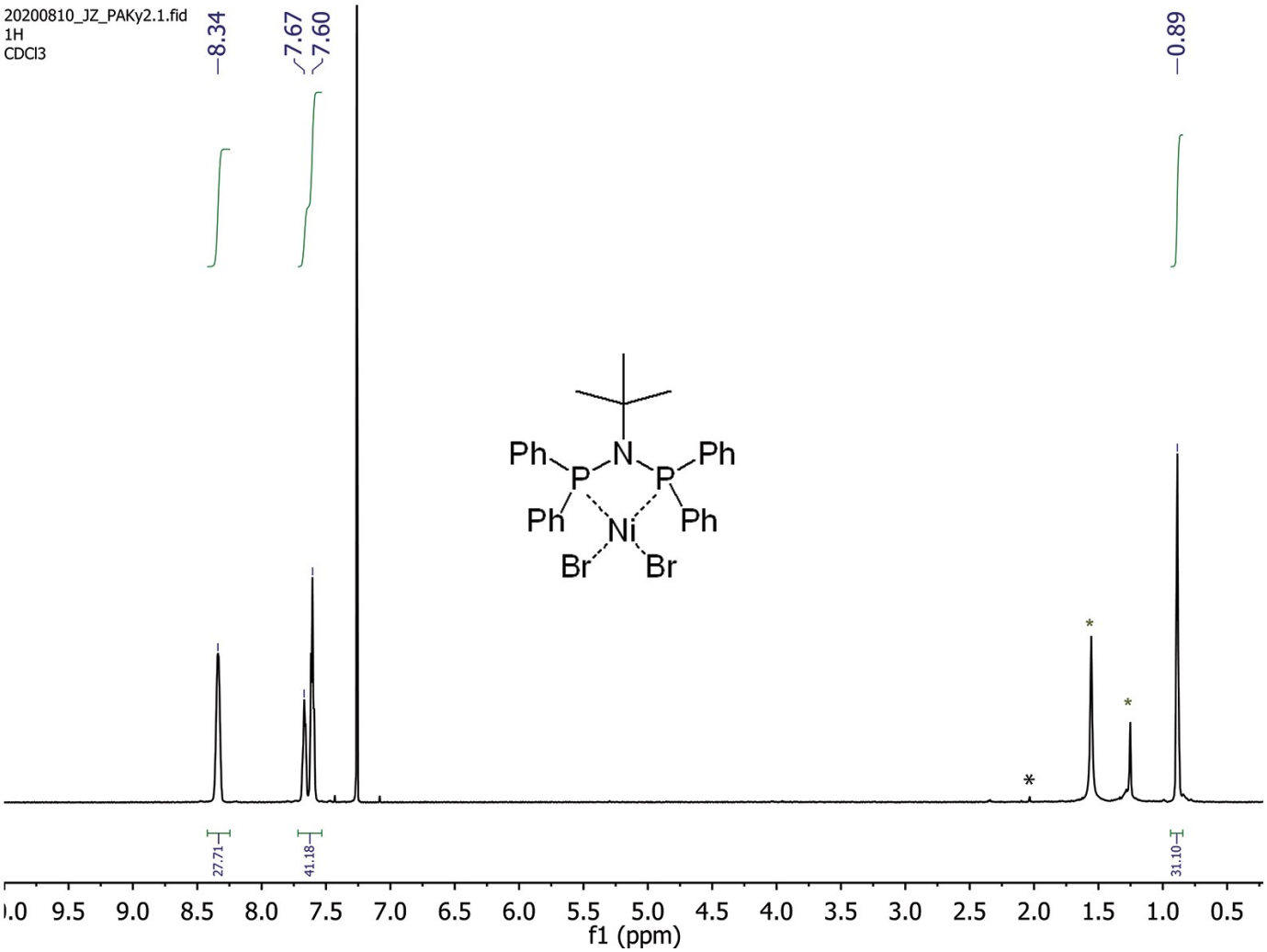

Figure S6. ^{1}H NMR (600 MHz, $CDCl_3$) spectrum of **[Ni(P,P)Br$_2$]**. S – 7.25 ppm CH_3Cl (solvent signal), 2.1 ppm – acetone,1.50 ppm trace of moisture, 1.25 ppm trace of hexane, all impurities are marked by an asterisk.

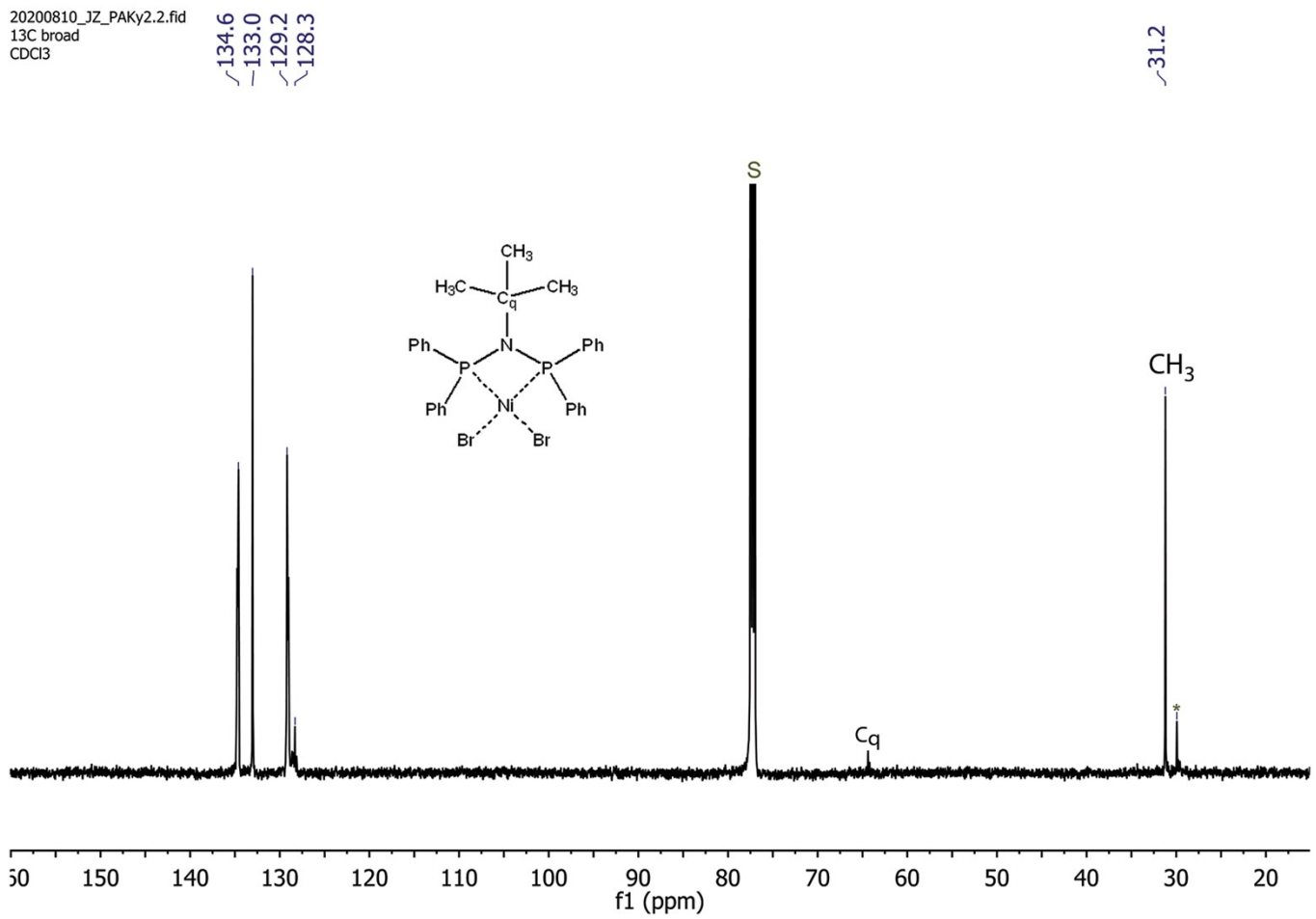

Figure S7. ^{13}C NMR (151 MHz, $CDCl_3$) spectrum of **[Ni(P,P)Br$_2$]**. S – solvent peak, residual trace of acetone (29.9 ppm) is marked by an asterisk.

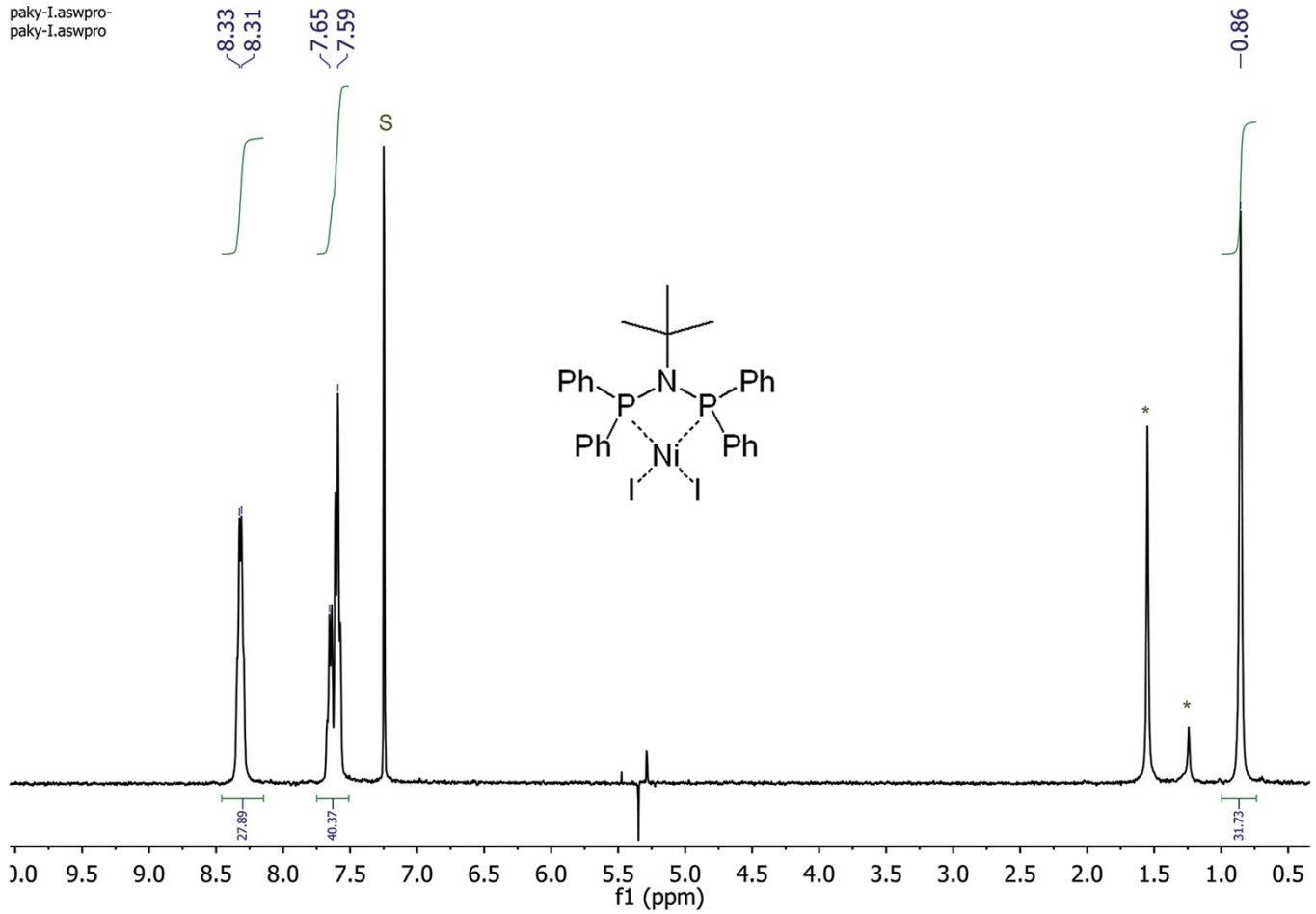

Figure S8. ^{1}H NMR (400 MHz, $CDCl_3$) spectrum of **[Ni(P,P)I_2]**. S – 7.25 ppm CH_3Cl (solvent signal), 1.50 ppm moisture, 1.25 ppm trace of hexane, all impurities are marked by an asterisk.

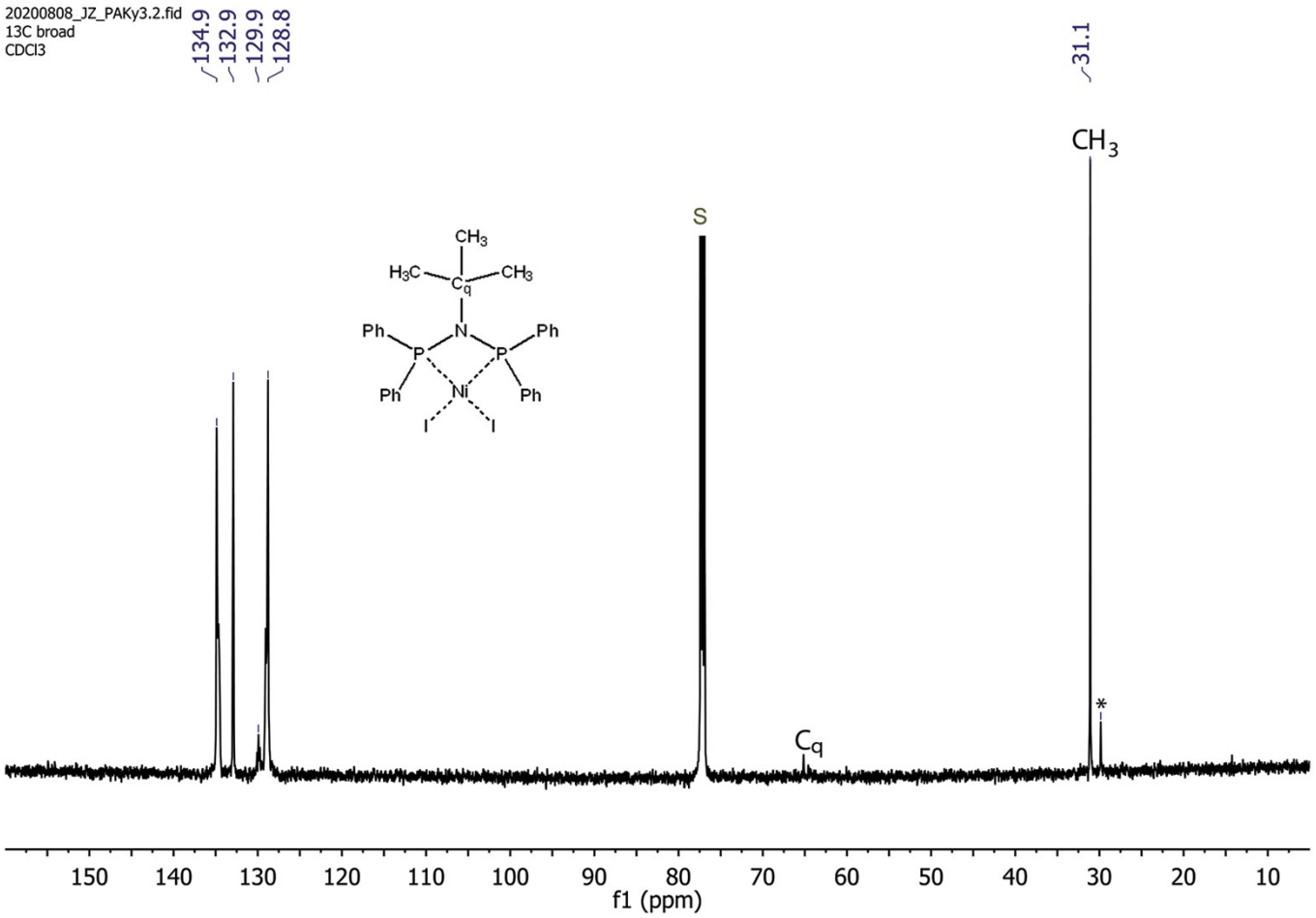

Figure S9. ^{13}C NMR (151 MHz, $CDCl_3$) spectrum of **[Ni(P,P)I_2]**, S – solvent peak, trace of acetone (29.9 ppm) is marked by an asterisk.

^{31}P NMR spectra

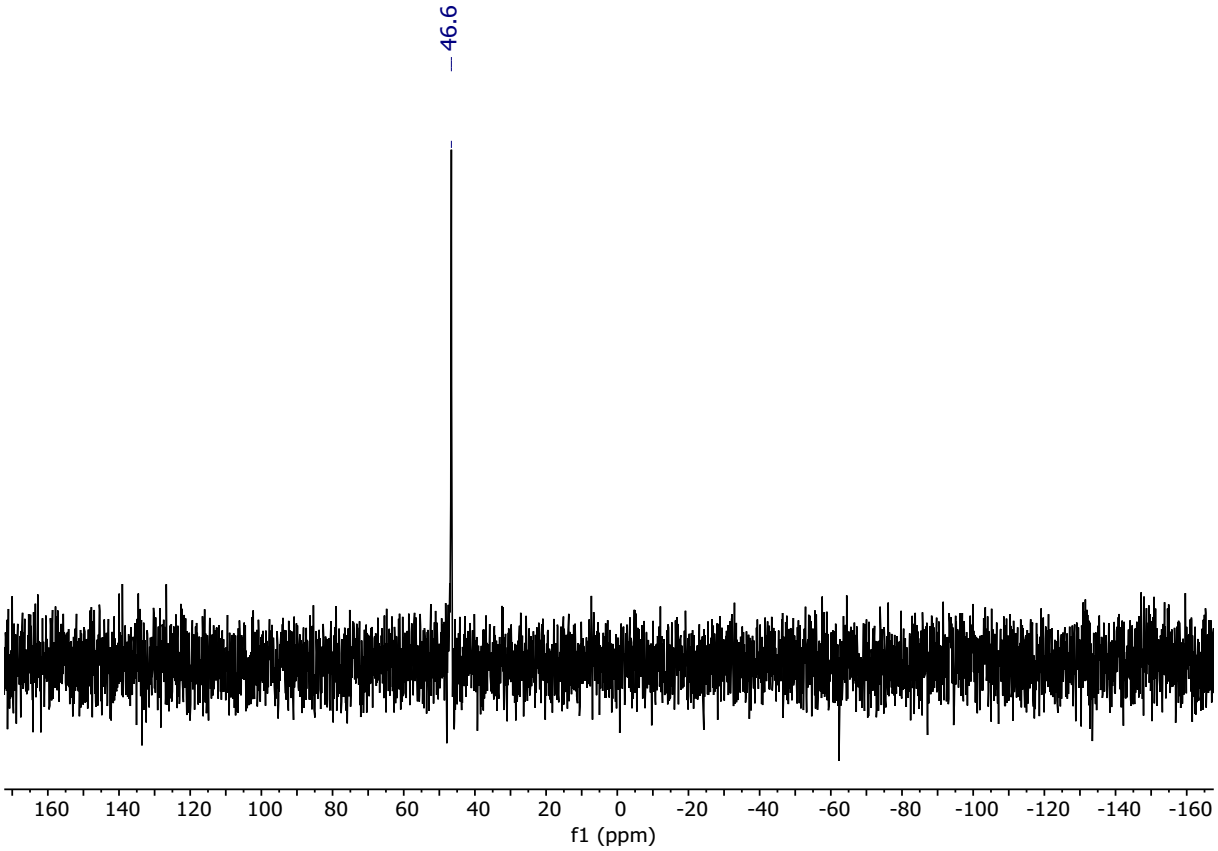

Figure S10. ^{31}P NMR (162 MHz, $CDCl_3$) spectrum of **[Ni(P,P)Cl$_2$]**. The spectral window was extended to the full scale.

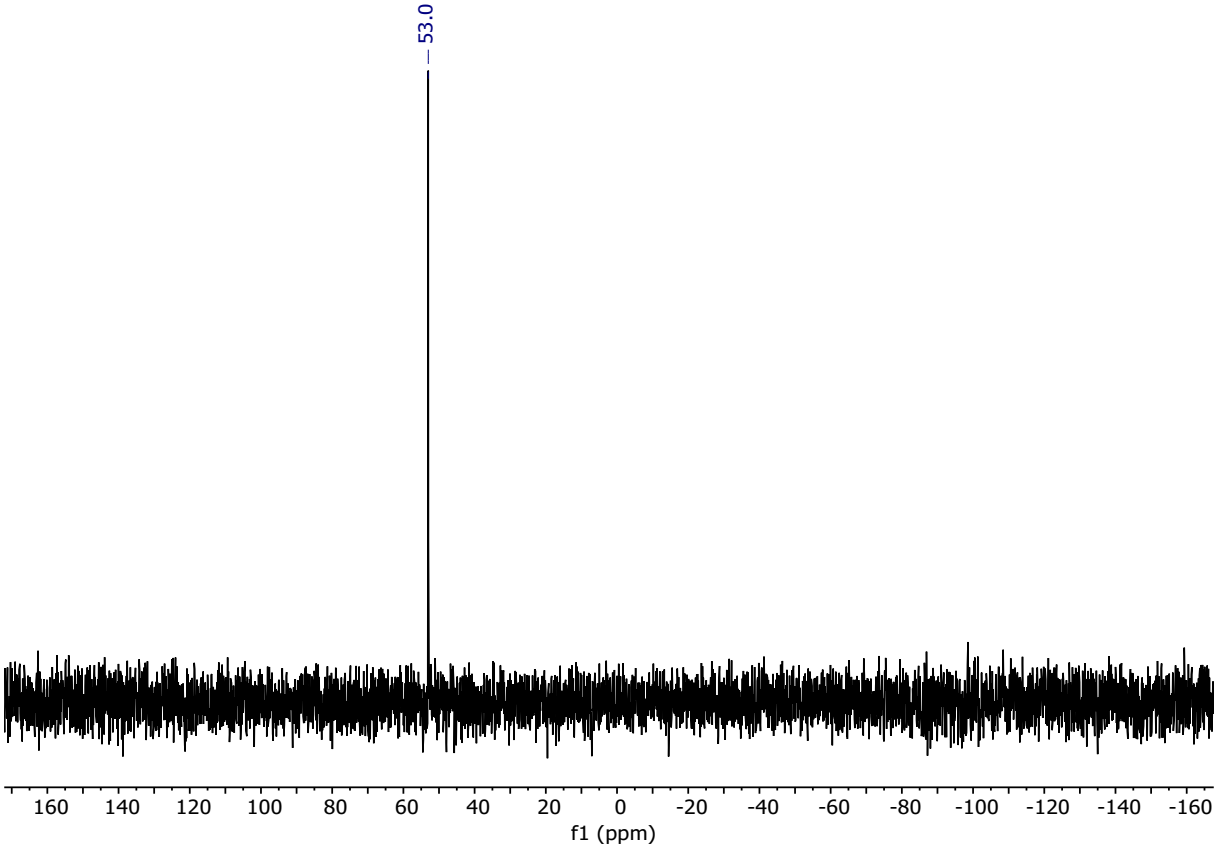

Figure S11. ^{31}P NMR (162 MHz, $CDCl_3$) spectrum of **[Ni(P,P)Br$_2$]**. The spectral window was extended to the full scale.

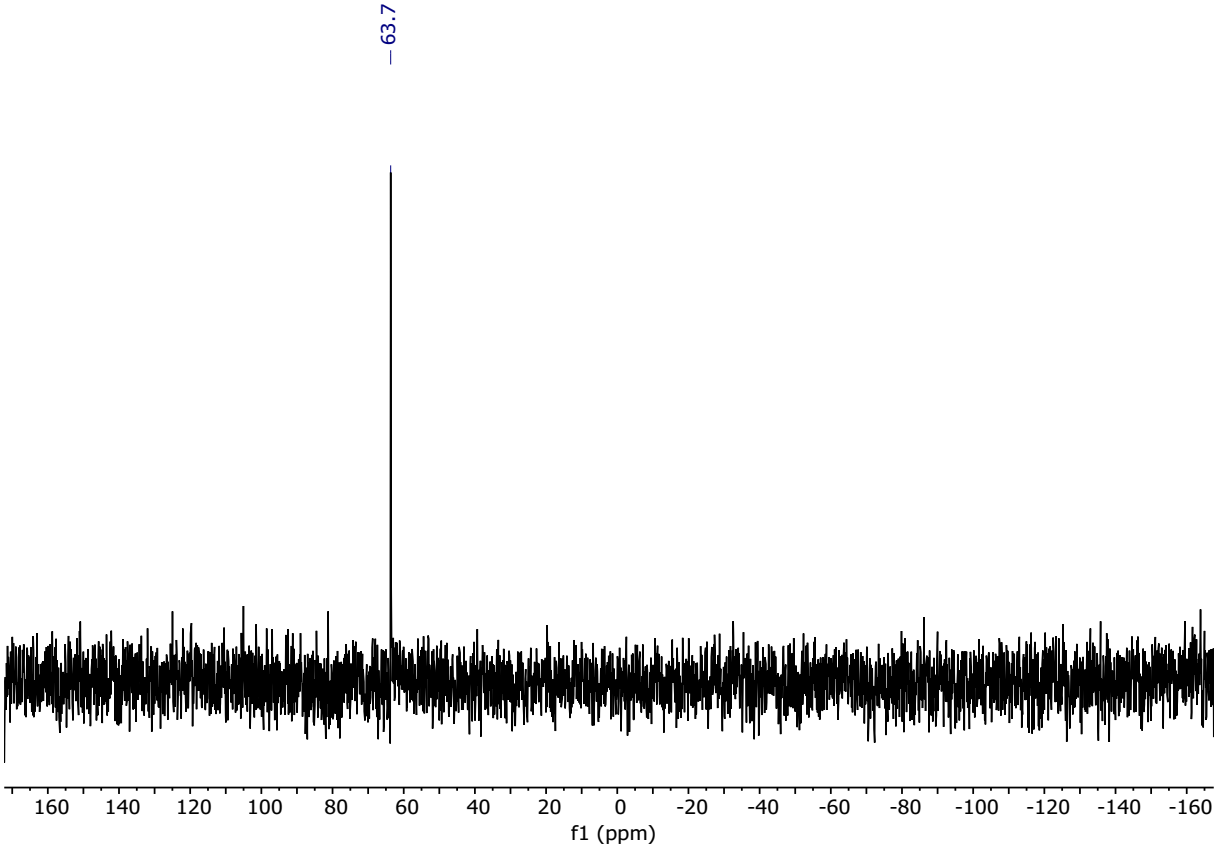

Figure S12. ^{31}P NMR (162 MHz, $CDCl_3$) spectrum of **[Ni(P,P)I$_2$]**. The spectral window was extended to the full scale.

X-ray crystallography

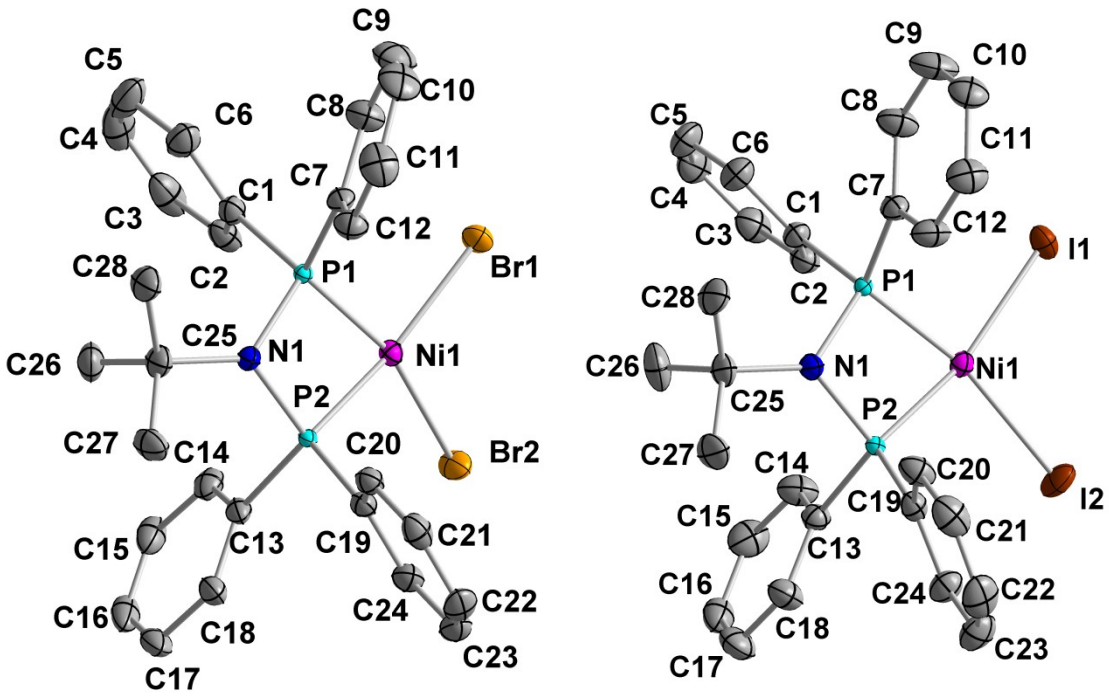

(a) (b)

Figure S13. Molecular structures and atom numbering of **[Ni(P,P)X_2]**, X = Br, I: (a) and (b), respectively**.** Thermal ellipsoids are presented at a level 50 % probability. Hydrogen atoms are omitted for clarity.

MS spectra

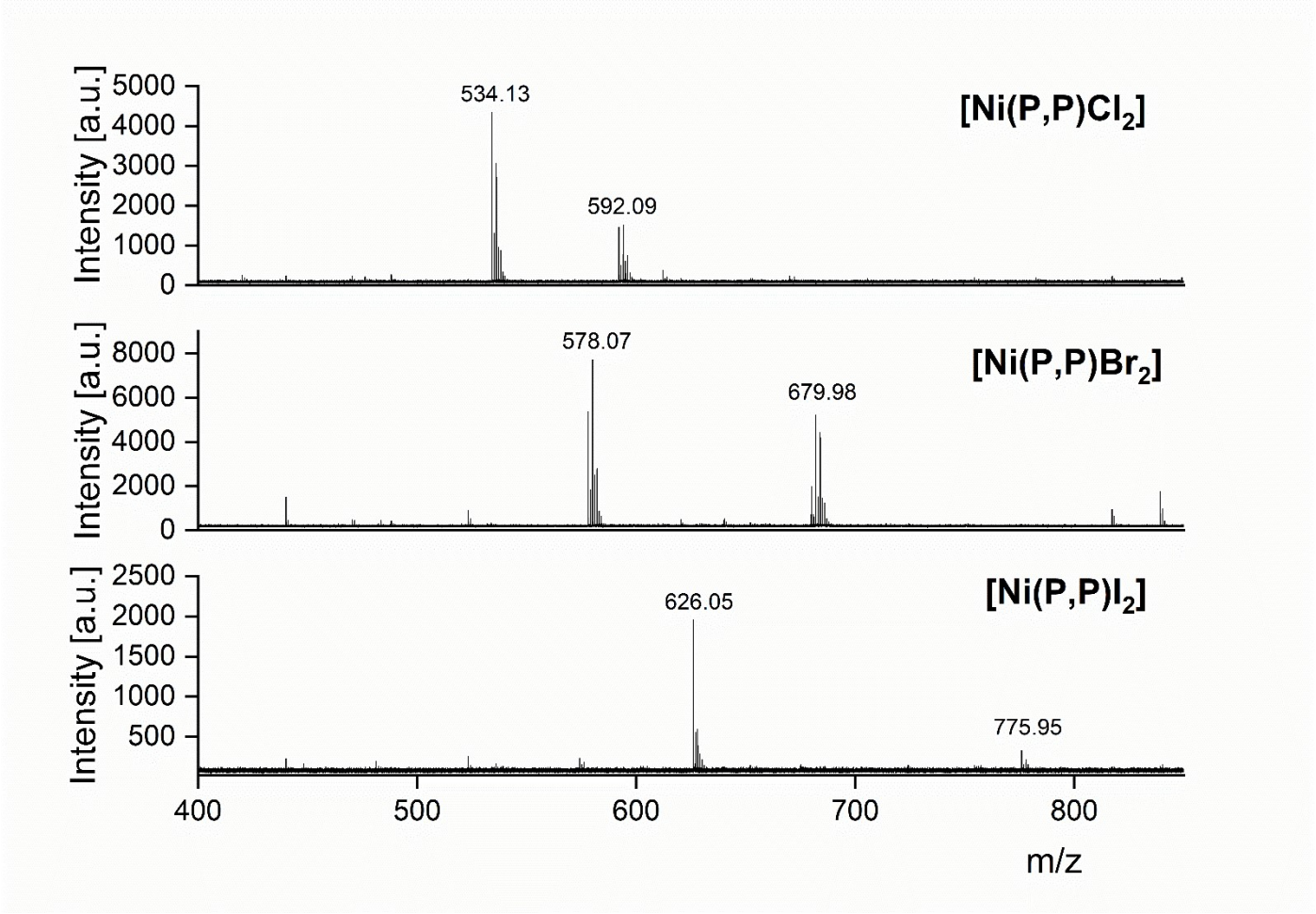

Figure S14. LDI-MS spectra of **[Ni(P,P)X_2]**.

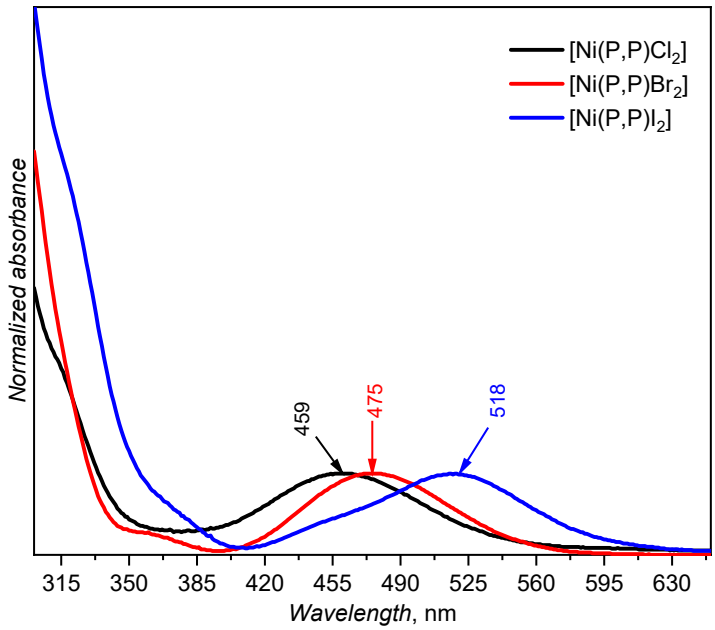

Figure S15. UV-vis spectra of complexes **[Ni(P,P)X_2]**, X = Cl (1), Br (2), I (3), in THF solution (~ 10^{-5} M)

Table S1. Data for reactions of **4-^{t}Bu** substrate with Grignard reagent **T** catalyzed by complexes **[Ni(P,P)X$_2$]**. Y_{CROSS} and Y_{HOMO} stand for the substrate conversion by cross-coupling and homo-coupling, respectively (Scheme 2).

[Ni(P,P)X$_2$] Catalyst		X = Cl		X = Br		X = I	
Reaction	*t*, min	Y_{CROSS} %	Y_{HOMO} %	Y_{CROSS} %	Y_{HOMO} %	Y_{CROSS} %	Y_{HOMO} %
4-^{t}Bu + T	20	76	< 2	1.0	< 2	1	< 2
	90	85	< 2	51	< 2	22	< 2
	1080	90	< 2	61	< 2	65	< 2

Table S2. Data for Kumada coupling reactions between substrates with shielded iodine atom and Grignard reagent **T** catalyzed by **[Ni(P,P)Cl$_2$]**. Y_{CROSS} and Y_{HOMO} stand for the substrate conversion by cross-coupling and homo-coupling, respectively (Scheme 2).

Substrate		**4-^{t}Bu**		**2-Me**		**2,6-diMe**	
Catalyst	*t*, min	Y_{CROSS} %	Y_{HOMO} %	Y_{CROSS} %	Y_{HOMO} %	Y_{CROSS} %	Y_{HOMO} %
[Ni(P,P)Cl$_2$]	20	76	< 2	20	8	57	18
	90	85	< 2	73	12	58	24
	1080	90	< 2	76	15	62	26

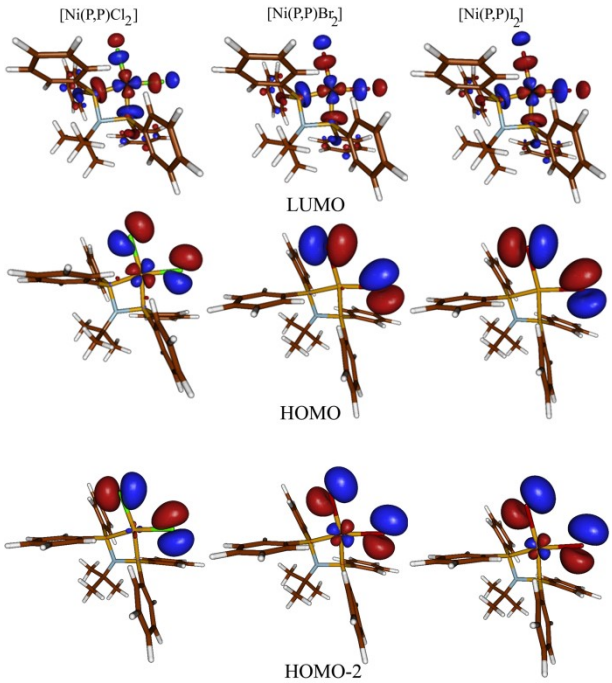

Figure S16. The DFT-calculated LUMO, HOMO and HOMO-2 orbitals of complexes **[Ni(P,P)X$_2$]** showing contours at ±0.05 a.u.

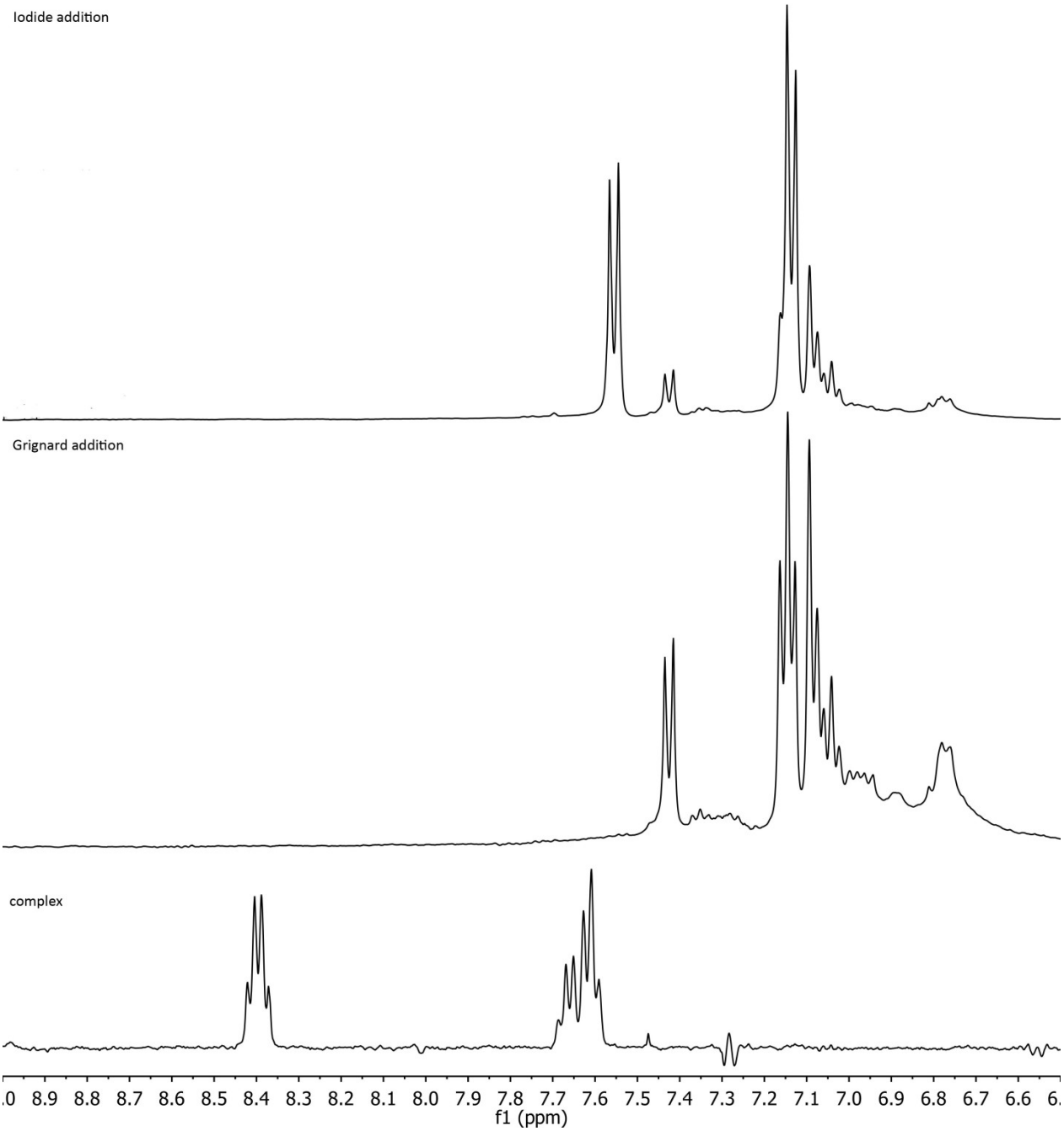

Figure S17. ^{1}H NMR spectra upon addition of first **T** and then **4-^{t}Bu** to a THF solution of **[Ni(P,P)Cl$_2$]**.

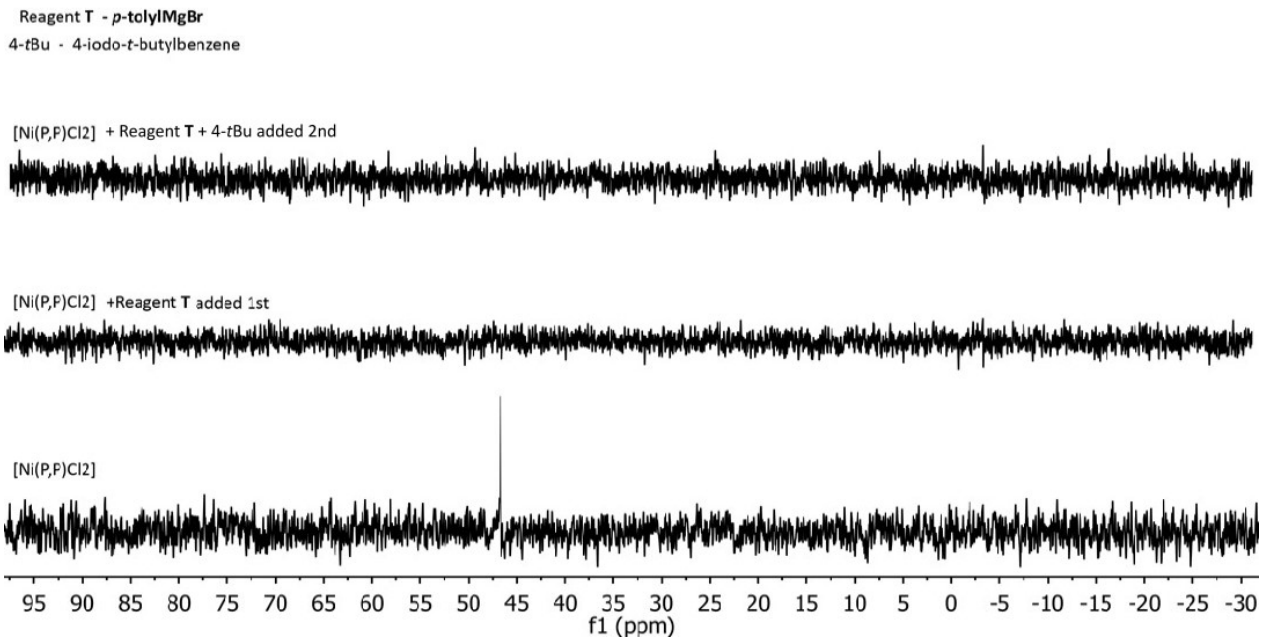

Figure S18. ^{31}P NMR spectra upon upon addition of first **T** and then **4-^{t}Bu** to a THF solution of **[Ni(P,P)Cl$_2$]**.